

Translate. Create. Deliver.

NORTHERN TERRITORY SOLAR RESOURCE PROJECT HANDLING VARIABILITY WITH HIGH QUALITY GROUND STATION DATA

Date: July 2021

Prepared for: Northern Territory Government



About Ekistica

Ekistica is a professional advisory and technical consultancy firm based in Central Australia.

We deliver innovative solutions to the complex challenges of remote area infrastructure development through a diverse team of more than twenty professional engineers, project managers, engagement specialists and data analysts.

We provide high quality, independent advice, project development, engineering design and project delivery services for a wide range of infrastructure and related services, to clients that include state and national governments, intergovernmental agencies, power utilities, community service organisations, large commercial firms and private investment firms.

Disclaimer

Ekistica Pty Ltd, ABN 74 126 787 853

© Ekistica 2021

This document is and shall remain the property of Ekistica. The document may only be used for the purposes for which it was prepared. Any unauthorised use of this document is expressly prohibited.

Executive Summary

This report presents the findings of analysis of the long-term and short-term variability of solar resource in the Northern Territory carried out using the high quality, high resolution data collected by the Northern Territory Solar Resource project.

The Northern Territory Solar Resource (NTSR) project funded the installation of four Class A ground stations meeting IEC 61724-1 to provide freely and easily accessible, high-quality, ground-based solar resource data. One of the key objectives of the project was to reduce the barriers to investment in large-scale solar projects throughout the Northern Territory (NT). The stations were installed in Darwin, Katherine, Tennant Creek and Alice Springs, representing the range of climate zones across the Territory, and were completed and commissioned in May 2019.

With at least 11 months of data now collected at each of the stations, this study demonstrates the value of the high quality, high resolution NTSR project data by illustrating how the data can be used to quantify the long-term and short-term variability of solar resource in the NT, thereby reducing the risk associated with PV system installations.

To quantify long-term variability for PV feasibility studies, long-term satellite datasets are typically used, as ground station data is rarely available. The procedure of site adaptation can be used to correct satellite datasets for site-specific biases and reduce the uncertainty associated with the expected annual insolation estimates. This requires an overlapping period of high-quality ground station data.

A site adaptation procedure was carried out on the NASA POWER satellite irradiance data for each of the four sites using the NTSR project data as the ground station reference. The application of this methodology increased the 1-year P90 annual global horizontal insolation (GHI) estimates at the different sites by up to 28%. This illustrates the capacity of the ground station data to reduce the risk associated with long-term variability of solar resource for a given project.

The high resolution of the NTSR project data can also assist developers managing the risks associated with short-term variability of solar resource data. One application is the optimising of battery energy storage system (BESS) sizing to support forecasting at the level of accuracy required to meet current performance standards.

An implementation of this methodology illustrated that the optimal BESS size increased with the increasing short-term irradiance variability, as observed at the Top End stations. More conservative forecasts also resulted in larger BESS sizes required to maximise value. Assuming a 'mid-range' forecast accuracy representative of current cloud forecasting technology, the optimal BESS size for a 1 MW solar farm ranges from 710 kW in Darwin to 610 kW in Alice Springs.

Finally, the fact that these long-term and short-term variability analyses produced markedly different results for each of the four sites demonstrates the value of having consistent high quality ground stations distributed across the distinct climate zones across the NT.

ABBREVIATIONS

| Abbreviation | Definition |
|--------------|---|
| BESS | Battery Energy Storage System |
| DKASC | Desert Knowledge Australia Solar Centre |
| GHI | Global Horizontal Irradiance |
| MBE | Mean Bias Error |
| NPV | Net Present Value |
| NTG | Northern Territory Government |
| NTSR | Northern Territory Solar Resource (Project) |
| RMSE | Root Mean Square Error |
| PV | Photovoltaic |
| PWC | Power and Water Corporation |

Table of contents

| | |
|--|-----|
| Abbreviations | iii |
| Glossary | 1 |
| 1 Introduction | 2 |
| 2 Long-Term Variability | 3 |
| 2.1 Overview | 3 |
| 2.2 Site Adaptation | 3 |
| 2.2.1 Methodology | 4 |
| 2.2.2 Results | 5 |
| 2.3 Quantifying and Reducing Uncertainty | 7 |
| 2.3.1 Measurement Uncertainty | 7 |
| 2.3.2 Interannual Variability | 8 |
| 2.3.3 Overall Uncertainty | 9 |
| 2.4 Application | 9 |
| 3 Short-term variability | 11 |
| 3.1 Overview | 11 |
| 3.2 Battery Sizing Methodology | 12 |
| 3.2.1 Background | 12 |
| 3.2.2 PV Profiles | 12 |
| 3.2.3 Forecasting | 13 |
| 3.2.4 Curtailment Calculation | 14 |
| 3.2.5 NPV Calculation | 15 |
| 3.3 results | 15 |
| 4 Conclusion | 18 |
| 5 References | 19 |

Figures

Figure 2-1 Daily profiles of GHI by season and location for NTSR stations.3

Figure 2-2 Monthly average of daily GHI from NASA POWER, corrected NASA POWER and ground station measurements for Alice Springs.5

Figure 2-3 Error in GHI measurements for Alice Springs, satellite versus ground station, before (top) and after (bottom) site adaptation 6

Figure 2-4 Effect of site adaptation on long-term uncertainty.....10

Figure 3-1 Irradiance ramp rate distributions at NTSR project sites 11

Figure 3-2 Simulated forecasts on selected days 14

Figure 3-3 PV and battery operation illustration with the Mid-Range Forecast15

Figure 3-4 Optimal BESS sizing results 16

Tables

Table 2-1 Site Adaptation Model Performance6

Table 2-2 Standard Measurement Uncertainty.....8

Table 2-3 Combined Standard Uncertainty9

Table 2-4 Raw vs Site Adapted P50 and P90 values 10

Table 3-1 Simulated Sky-Camera Forecasts.....13

Table 3-2 Optimal BESS size for PV firming 17

GLOSSARY

| Term | Description |
|--|---|
| Mean Bias Error (MBE) | $MBE = \frac{\sum_{i=1}^n error_i}{n}$ <p>Where:</p> $error_i = y_{model,i} - y_{actual,i}$ <p>Indicates whether a model consistently overestimates or underestimates the target value.</p> |
| Standard Deviation of Bias (SD) | $SD = \sqrt{\frac{\sum_{i=1}^n (error_i - \overline{error})^2}{n}}$ <p>Indicates the variation in the bias over the modelled values. Where there are more than approximately 30 values, this can be taken as the population standard deviation.</p> |
| Root Mean Square Error (RMSE) | $RMSE = \sqrt{\frac{\sum_{i=1}^n (error_i)^2}{n}} = \sqrt{MBE^2 + SD^2}$ <p>Measures the average error of model without considering error direction and gives a relatively high weight to large errors. Reflects both the bias and variation in the error of the dataset.</p> |
| Standard Uncertainty (u) | The standard uncertainty associated with an estimate of a quantity, equal to one standard deviation. This can be expressed as an absolute value or as a percentage of the mean value of the quantity being estimated. |
| Expanded Uncertainty (U) | $U = ku$ <p>The uncertainty associated with an estimate at a given confidence level. The standard uncertainty can be converted to an expanded uncertainty using a coverage factor, k. Where the uncertainty follows a normal distribution, coverage factor is approximately k = 2 for a 95% confidence level.</p> |
| Y-year PXX Estimate | <p>An estimate for a value that will be exceeded in XX% of observations of the value over a Y-year period. For example:</p> <ul style="list-style-type: none"> • If the 1-year P50 estimate of the total annual global horizontal irradiance (GHI) is 2000 kWh/m², the probability that the total GHI in any given year exceeds 2000 kWh/m² is 50%. • If the 10-year P90 estimate of the total annual GHI is 1900 kWh/m², the probability that the average annual total GHI over a 10-year period exceeds 1900 kWh/m² is 90%. |

1 INTRODUCTION

The Northern Territory Government (NTG) has a Renewable Energy Target of 50% by 2030 [1]. While small and medium-scale solar power use has a long history in the Northern Territory (NT), investment in utility-scale renewables was lagging other states in 2017 [2]. This is despite the Territory's excellent solar resource and ample land available for solar farm development.

To assist in addressing the gap between opportunity and investment towards the 2030 target, the Northern Territory Solar Resource (NTSR) project was funded by the NTG and the Intyalheme Centre for Future Energy.

The NTSR project has installed four Class A ground stations meeting IEC 61724-1 with the aim of providing freely and easily accessible, high-quality, ground-based solar resource data, so that potential developers and investors are better equipped to manage solar resource risk, one of the key risks in financial models for utility-scale PV [3].

The meteorological stations were installed in Darwin, Katherine, Tennant Creek and Alice Springs, representing the range of climate zones across the Territory [2]. Installation and commissioning of the four sites reached completion in May 2019, with all sites in operation, measuring and transferring high resolution data. The following variables are sampled every second and averaged into five-second intervals: global horizontal irradiance (GHI), global plane-of-array irradiance, direct normal irradiance (except at the Darwin station), wind speed and direction, ambient temperature, relative humidity, and rainfall. Data collected at each site is automatically uploaded to a free, open-access web page, hosted through the Desert Knowledge Australia Solar Centre (DKASC) website.

This report considers two specific use cases for this dataset to better understand solar resource variability at different locations in the NT for the de-risking of potential investment in large-scale PV projects.

First, the dataset provides a high-quality ground-based dataset to complement long-term satellite datasets. Through site adaptation procedures, this enables more accurate estimates of interannual irradiance variability to be calculated. Second, the high frequency data can be used to optimise battery energy storage sizing for PV firming to meet current forecasting requirements in the different climate zones.

2 LONG-TERM VARIABILITY

2.1 OVERVIEW

Expected variability of irradiance conditions over long time scales is a crucial input for large-scale solar project financial models. Over time, the NTSR project will become a source of high-quality data on the distribution of monthly and annual insolation throughout the NT. At the time of writing, more than one year of data has been collected from each of the sites (with the exception of Tennant Creek, which has 11 months of data available).

The figure below summarises the plane-of-array irradiance data captured to date and the utility of the dataset in characterising seasonal profiles.

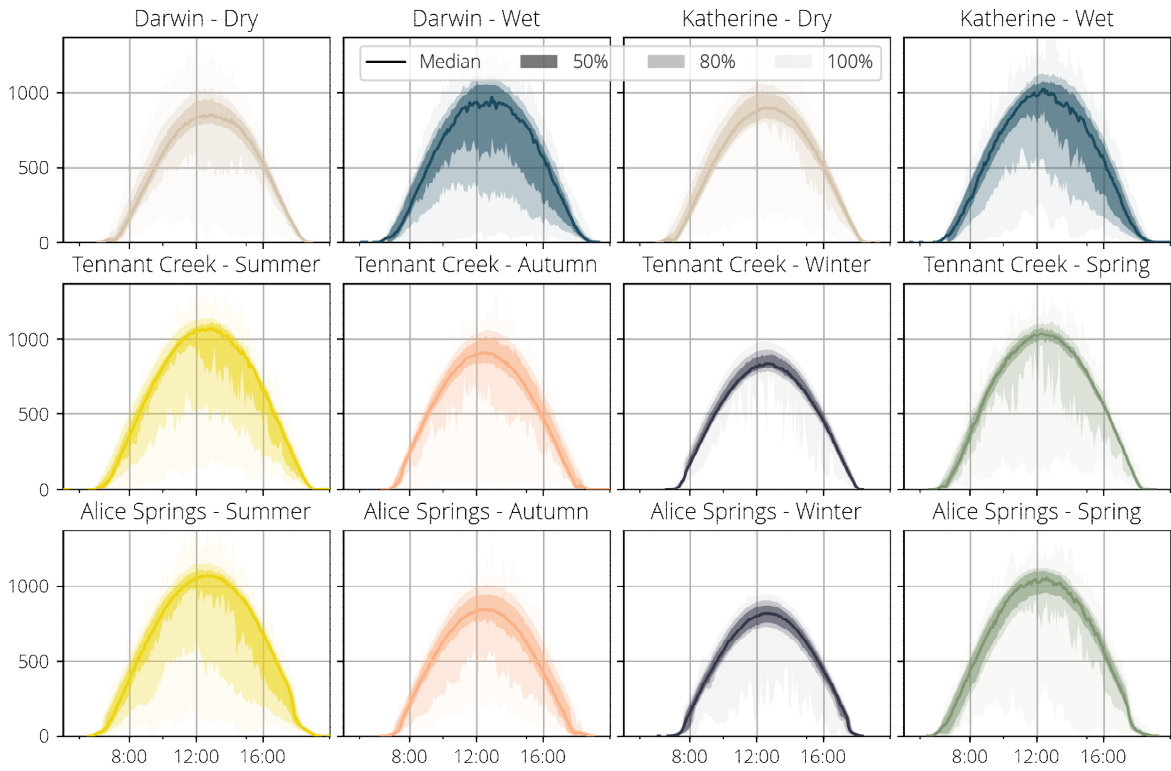


Figure 2-1 Daily profiles of GHI by season and location for NTSR stations.

The percentage bands indicate the range between which the specified proportion of the dataset falls about the median, eg, the 50% band spans from the 25th to the 75th percentile.

These plots show the distinct climates at the different locations, especially the significantly greater degree of irradiance variability experienced in tropical locations during the wet season relative to other sites, as expected.

2.2 SITE ADAPTATION

Being only established in 2019, the NTSR projects cannot as yet provide a sufficiently long time series to enable the characterisation of interannual variability at each location,

however, they can be combined with satellite data to improve long-term estimates through the process of site adaptation.

“Site adaptation” refers to the correction of long-term satellite estimated irradiance datasets using ground-measured data. This practice is also known as “measure, correlate, predict” in the wind energy industry.

Below, the site adaptation of GHI values is demonstrated for each location using the NTSR project data and satellite measurements from the NASA POWER project. This analysis shows how the NTSR project data can be used to:

- Improve the accuracy of P50 GHI estimates.
- Reduce the uncertainty in estimates of interannual variability.

2.2.1 Methodology

Multiple industry standard methods exist for identifying and correcting the bias found in satellite datasets using high quality ground station measurements, summarised in detail in [4] and discussed in the National Renewable Energy Laboratory (NREL) *Best Practices Handbook for the Collection and Use of Solar Resource Data for Solar Energy Applications: Second Edition* [5].

These methods are generally corrections of the variables of interest or the input parameters (such as clearness index or aerosol optical depth (AOD)), using simple scaling factors, linear regression, empirical quantile mapping, or other more complex methods. Model performance is typically evaluated based on the mean bias error (MBE) and root mean square error (RMSE) [5].

The approach used for site adaptation of satellite irradiance data in this study is as follows:

1. Calculate the clearness index for both satellite and ground station datasets.
2. Fit a linear regression model for the ground station clearness index based on satellite clearness index and time-dependent variables accounting for seasonal effects.
3. Calculate corrected satellite clearness index using the model from step 2.
4. Re-calculate satellite data based on the adjusted corrected clearness index.
5. Evaluate model to confirm that both MBE and RMSE are reduced under repeated 10-fold cross validation.

Multiple models were evaluated to determine the combination of covariates that minimised the MBE and RMSE under cross-validation. The covariates considered in addition to the clearness index were the apparent zenith, apparent elevation, and harmonic regression terms. The site adaptation of GHI measurements was ultimately carried out using the following linear model:

$$k_{GHI,met} \sim \beta_0 + \beta_1 k_{GHI,sat} + \beta_2 \alpha_e + \epsilon$$

Where:

- $k_{GHI,met} = \frac{GHI_{met}}{GHI_{clear}}$ = ground station GHI clearness index: ratio of observed GHI to GHI expected on a cloudless day for the solar position at the relevant timestamp and location (calculated using PVLIB).

- $k_{GHI,sat} = \frac{GHI_{sat}}{GHI_{clear}}$ = satellite GHI clearness index: ratio of GHI from satellite measurements observed at the ground station to GHI expected on a cloudless day for the solar position at the relevant timestamp and location (calculated using PVLIB).
- α_e = solar elevation angle calculated for the relevant timestamp and location, accounting for atmospheric refraction (calculated using PVLIB).
- ϵ = residual error in the model, assumed to be normally distributed.

The procedure above was applied to the NASA POWER satellite dataset. These data were obtained from the NASA Langley Research Center (LaRC) POWER Project funded through the NASA Earth Science/Applied Science Program.

2.2.2 Results

The figures below show how the monthly average daily insolation from the satellite dataset is brought closer to the value derived from ground station measurements following the site adaptation procedure.

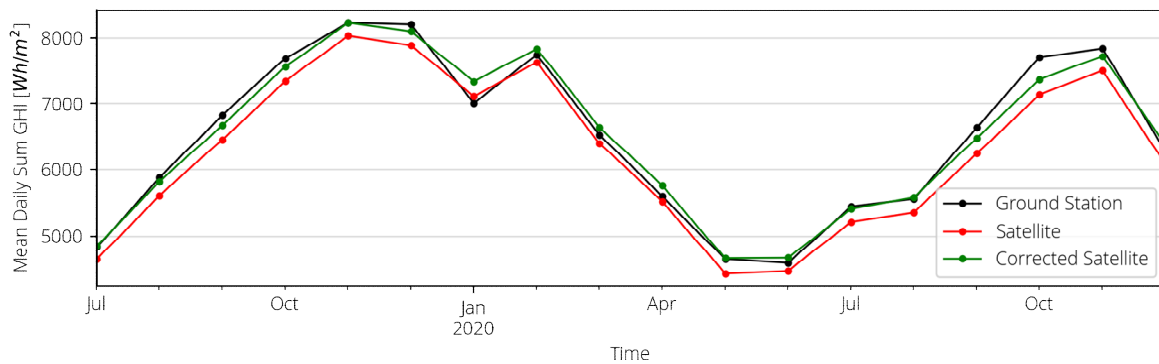


Figure 2-2 Monthly average of daily GHI from NASA POWER, corrected NASA POWER and ground station measurements for Alice Springs.

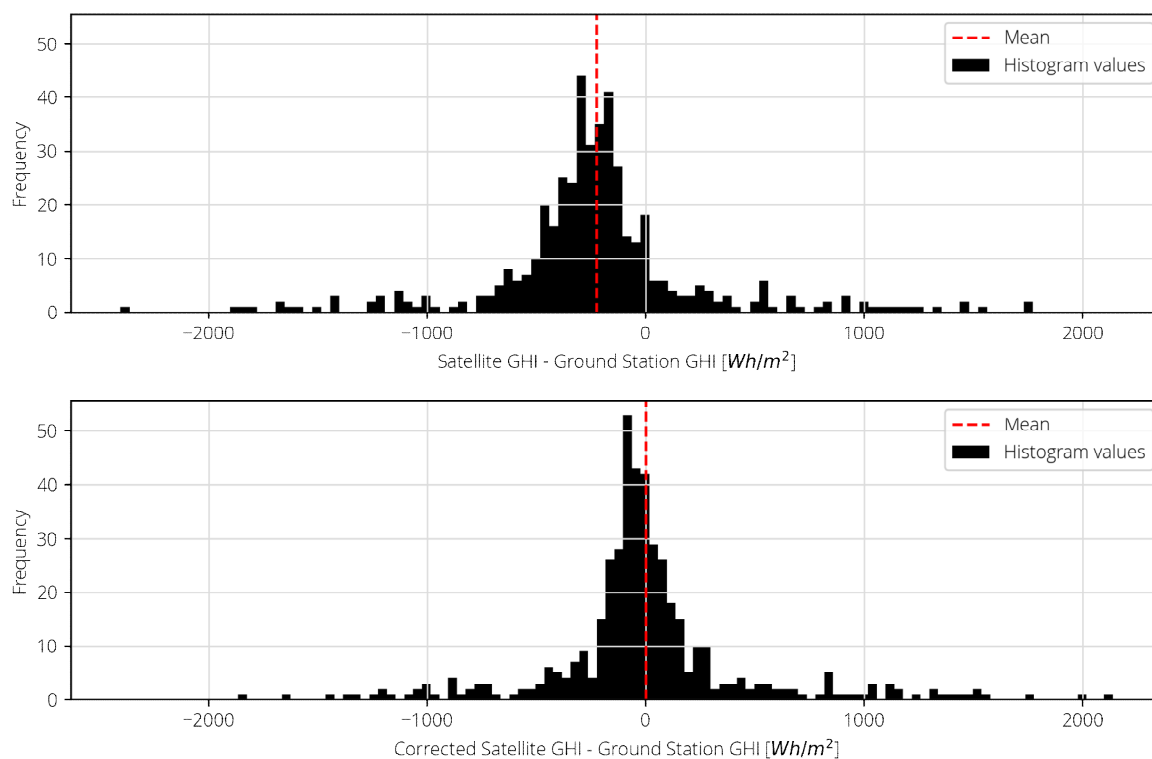


Figure 2-3 Error in GHI measurements for Alice Springs, satellite versus ground station, before (top) and after (bottom) site adaptation

The MBE and RMSE metrics for each model were calculated using 10 repetitions of 10-fold cross-validation to ensure that the model would reduce the error in satellite data values outside the training dataset [6].

Table 2-1 Site Adaptation Model Performance

| | Raw | Site Adapted | Change [%] |
|--|-------|--------------|------------|
| Darwin | | | |
| Mean Annual Total GHI [kWh/m²] | 2154 | 2086 | -3.16 |
| MBE [%] | 3.14 | 0.03 | -99.05 |
| RMSE [%] | 10.89 | 9.75 | -10.47 |
| Katherine | | | |
| Mean Annual Total GHI [kWh/m²] | 2186 | 2262 | 3.5 |
| MBE [%] | -2.98 | 0.07 | -102.32 |
| RMSE [%] | 8.24 | 7.25 | -12.03 |

| | Raw | Site Adapted | Change [%] |
|---|-------|--------------|------------|
| Tennant Creek | | | |
| Mean Annual Total GHI [kWh/m ²] | 2214 | 2279 | 2.94 |
| MBE [%] | -2.91 | -0.01 | -99.55 |
| RMSE [%] | 7.55 | 6.18 | -18.11 |
| Alice Springs | | | |
| Mean Annual Total GHI [kWh/m ²] | 2167 | 2252 | 3.93 |
| MBE [%] | -3.45 | -0.01 | -99.69 |
| RMSE [%] | 8.19 | 7.3 | -10.93 |

2.3 QUANTIFYING AND REDUCING UNCERTAINTY

There are two sources of uncertainty in the P50 GHI estimates: measurement uncertainty in the recorded GHI values and interannual variability. The analysis below calculates the measurement uncertainty and determines the best estimate of a 50% probability of exceedance value in the context of non-normally distributed interannual variability.

2.3.1 Measurement Uncertainty

Using the raw satellite data, the 1-year P50 total annual GHI estimate can be obtained for each site. The uncertainty associated with this value can be approximated using the daily error values provided by NASA POWER [7]. Given that annual insolation values tend to have much lower uncertainty than daily values, this can be considered an upper bound for the uncertainty [8, 9]. This is a standard uncertainty measurement, equivalent to one standard deviation from the mean.

The new P50 total annual GHI estimate is based on the site adapted satellite data sources. The uncertainty in these data sources can be calculated from the residual site-specific error in the dataset relative to ground station data, and the underlying uncertainty of the ground station measurements [8, 9]. In accordance with the JCGM's *Guide to the expression of uncertainty in measurement* [10], the measurement uncertainty in the site adapted satellite dataset can be calculated as per Equation 1 [5, 9] cf. [8].

Equation 1. Measurement Uncertainty for Site-Adapted Satellite Data

$$u_{\text{measurement}} = \sqrt{u_{\text{instrument}}^2 + MBE_{\text{model}}^2 + RMSE_{\text{model}}^2}$$

Ground station measurements of GHI at each NTSR station are taken from Secondary Standard pyranometers, which generally have an expanded uncertainty of $\pm 2\%$ at a 95% confidence level for daily total GHI measurements, which equates to a standard uncertainty

of 1% ($u_{instrument}$). While it is likely that this error is reduced significantly when total annual irradiance is considered [8], the daily uncertainty can be used as an upper bound on the uncertainty [9].

The MBE and RMSE of the daily site adapted datasets for each station are used as a more robust, if conservative, estimate of the uncertainty given that there is only one data point at the annual level.

The table below shows the uncertainty values applicable to the satellite datasets with and without the use of the NTSR project data for site adaptation. Without the NTSR project data, uncertainty values provided by NASA POWER must be adopted. Following site adaptation with the NTSR project data, the MBE and RMSE results from the site adapted dataset can be used.

Table 2-2 Standard Measurement Uncertainty

| Dataset | Raw NASA POWER Data | Darwin Site Adapted | Katherine Site Adapted | Tennant Creek Site Adapted | Alice Springs Site Adapted |
|-----------------------|---------------------|---------------------|------------------------|----------------------------|----------------------------|
| $u_{instrument}$ [%] | - | 1.00 | 1.00 | 1.00 | 1.00 |
| MBE_{model} [%] | -1.72 | 0.03 | 0.07 | -0.01 | -0.01 |
| $RMSE_{model}$ [%] | 20.47 | 9.75 | 7.25 | 6.18 | 7.3 |
| $u_{measurement}$ [%] | 20.54 | 9.80 | 7.32 | 6.26 | 7.37 |

2.3.2 Interannual Variability

The interannual variability in annual GHI for a given location is generally accounted for by making a simplifying assumption that the variation in the available historical data is normally distributed, fitting a normal distribution to the data, and taking the mean of the historical annual totals as the P50 estimate [11, 12]. The standard deviation of the fitted normal distribution is taken as the standard uncertainty due to interannual variability ($u_{interannual\ variability}$). However, the assumption of normality should be formally tested, as several past studies have shown that annual GHI may deviate from a normal distribution at certain locations [13, 14] cf. [15]. Where the data is not normally distributed, it is recommended to use the empirical cumulative frequency distribution to characterise interannual variability and take the median as the P50 estimate [12].

In the present case, the normality of each of the datasets of total annual insolation values for each location from the site-adapted satellite data was tested using the Shapiro-Wilk (cf. [15]). The null hypothesis that the data was normally distributed could not be rejected for any of the locations as the tests returned p values greater than 0.05.

The standard uncertainty due to interannual variability in the original NASA POWER dataset is 3.07%. For the site adapted datasets, this value is 2.88% for Darwin, 2.35% for Katherine, 3.11% for Tennant Creek and 2.89% for Alice Springs.

2.3.3 Overall Uncertainty

The combined standard uncertainty for the P50 estimate is calculated per Equation 2 below.

Equation 2. Combined Uncertainty for Total Annual GHI P50 Estimate

$$u_{total} = \sqrt{u_{measurement}^2 + u_{interannual\ variability}^2}$$

Where:

- u_{total} = Combined standard uncertainty in P50 estimate, equivalent to one standard deviation.
- $u_{measurement}$ = Standard uncertainty of site adapted satellite records per Equation 1.
- $u_{interannual\ variability}$ = Standard uncertainty due to inter-annual variability, equal to the standard deviation of the observed annual totals in the satellite dataset.

The combined uncertainty for the raw NASA POWER dataset and the site adapted datasets are summarised in the table below.

Table 2-3 Combined Standard Uncertainty

| Dataset | Raw NASA POWER Data | Darwin Site Adapted | Katherine Site Adapted | Tennant Creek Site Adapted | Alice Springs Site Adapted |
|-----------------------------|---------------------|---------------------|------------------------|----------------------------|----------------------------|
| $u_{measurement}$ [%] | 20.54 | 9.80 | 7.32 | 6.26 | 7.37 |
| $u_{interannual\ var.}$ [%] | 3.07 | 2.88 | 2.35 | 3.11 | 2.89 |
| u_{total} [%] | 20.77 | 10.21 | 7.69 | 6.99 | 7.92 |

2.4 APPLICATION

The result of the site adaptation procedure is a long-term dataset for each site that has better accuracy and lower uncertainty than the raw satellite data. This is only possible due to the availability of the high-quality ground station data collected under the NTSR project.

This improved input data can be used as an input for feasibility studies that better capture the risk associated with solar resource at each location. The ratio of 1-year P50 and P90 annual irradiance values is often used as a baseline approximate quantification of the expected long-term variability at a site [1].

In this study, the site adaptation procedure increases the P90 estimates by approximately 14–28% across the 4 sites, through a combination of bias removal and reduced uncertainty (cf. [16]). The plots below further illustrate the combined effect of the site adaptation and uncertainty quantification procedure on the accuracy of the distribution of annual insolation for each site. The increase in the P90 solar resource estimate reflects a reduction in the perceived risk of a PV project in the corresponding location.

Further, the P50 estimate in Darwin is reduced as a result of site adaptation, while it is increased for the other three sites. This reflects a difference in the bias of satellite data for

the different locations and underscores the value of having ground station data in each of the four distinct latitudes across the NT.

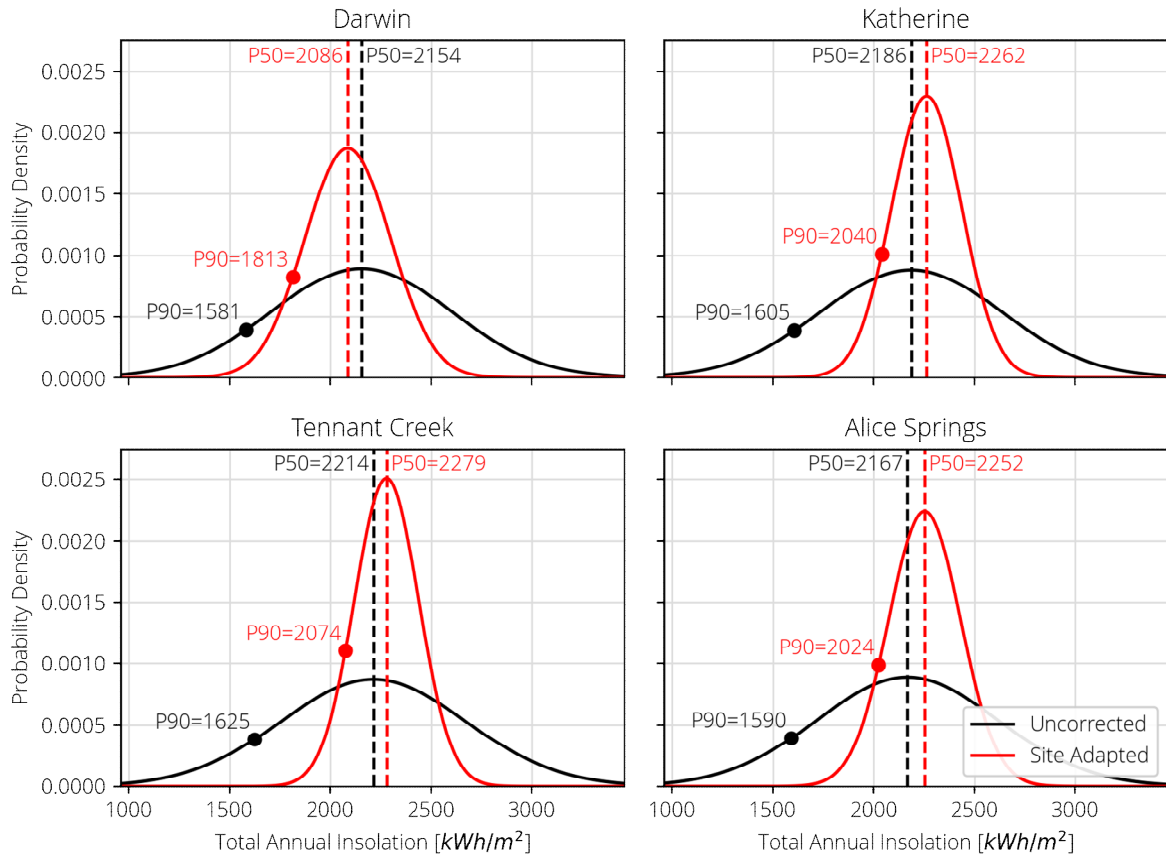


Figure 2-4 Effect of site adaptation on long-term uncertainty

The values are summarised in the table below.

Table 2-4 Raw vs Site Adapted P50 and P90 values

| | Raw | | Site Adapted | |
|----------------------|------|------|--------------|------|
| | P50 | P90 | p50 | P90 |
| Darwin | 2154 | 1581 | 2086 | 1813 |
| Katherine | 2186 | 1605 | 2262 | 2040 |
| Tennant Creek | 2214 | 1625 | 2279 | 2074 |
| Alice Springs | 2167 | 1590 | 2252 | 2024 |

3 SHORT-TERM VARIABILITY

3.1 OVERVIEW

Accurate characterisation of the short-term irradiance variability at a location is essential for accurately estimating likely curtailment and optimising technologies used for ramp-rate control and/or output smoothing such as batteries and cloud cameras [17]. The data from the NTSR project is provided at 5-second resolution, suitable for this type of application.

The graphs below demonstrate the probability density function of the 5 second, 1 minute and 5 minute ramp rates at each location over the observed data. This indicates the higher variability to be expected for PV generators in the Top End at higher time resolutions.

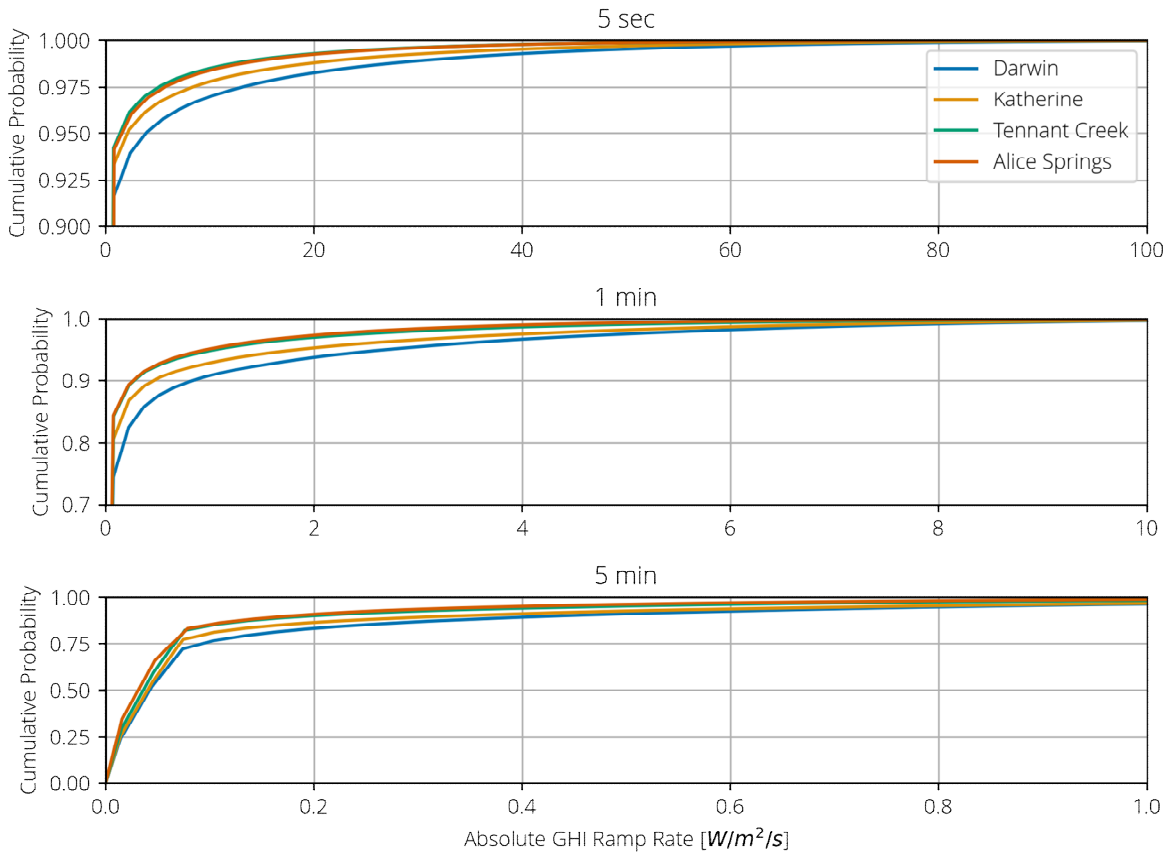


Figure 3-1 Irradiance ramp rate distributions at NTSR project sites

Below is an illustration of a specific application of the NTSR project data used to determine the optimal battery energy storage system (BESS) size for PV firming at each of the four project locations.

3.2 BATTERY SIZING METHODOLOGY

This section provides a methodology for determining a financially optimal firming solution (i.e., BESS sizing) for a large-scale PV array that meets the capacity forecasting requirements set out in Power and Water Corporation's (PWC's) Network Technical code. Among the goals of this analysis is to provide evidence for the hypothesis that the optimal battery size, and therefore project value of a compliant PV system, differs significantly across each of the NT's regulated systems (Darwin, Katherine, Tennant Creek, and Alice Springs), due to their differing climates.

3.2.1 Background

Power and Water Corporation's Network Technical Code [18], specifies the standards for generators seeking a license to connect to any of the Territory's regulated power systems. As of 29 February 2020, the code includes a requirement for all licensed generators, including large-scale solar PV, to provide a rolling 'Capacity Forecast'. The details of the forecasting requirement are defined in clause 3.3.5.17 of the code. The capacity forecasting automatic access standard in section 3.3.5.17(b) is as follows.

1. *Subject to paragraph (f), a Generator must supply to the Power System Controller a forward forecast of the capacity of its generating system.*
2. *The forecast in 3.3.5.17(b)(1) must. (i) include a 24 hour ahead forecast for capacity for every 5 minute interval, updated at 5 minute intervals; and (ii) have an accuracy such that in any rolling 24 hour period, at least 90% of the non-zero forecasts for the intervals commencing from $t=5$ to $t= 30$ do not exceed the firm offer for the time for which the forecast was made.*
3. *For the forecast updates that do not meet paragraph (2)(ii) above, that exceed the firm offer, the forecast must not exceed the firm offer by a margin greater than (i) 5% of the generating unit's nameplate rating; or (ii) 1 MW, whichever is the lesser.*
4. *The firm offer must be the capacity of the generating system for the interval and therefore the generating system must follow a dispatch instruction up to the firm offer in accordance with the requirements in clause 3.3.5.14. Note: When issuing dispatch instructions, the System Controller will respect plant limits such as firm offers and ramp rates of plant.*

The key result of this requirement is that PV generators will need to self-curtail to ensure that their capacity forecasts consistently achieve an accuracy of 90%. One way to avoid these curtailment losses is to install a BESS of sufficient size and capacity such that the BESS can dispatch power in intervals where the PV generation falls below the forecast.

3.2.2 PV Profiles

The PV profiles in this analysis have been generated using the PVLIB Python library, assuming a 1 MW, single-axis tracking array with a 1.2 DC-to-AC ratio. The NTSR data for DNI (except for Darwin) and GHI were used as inputs to the PVLIB profile generation function. The clear sky PV profile was also generated using PVLIB [19].

3.2.3 Forecasting

With less accurate forecasting, the PV is operated more conservatively and more heavily curtailed. To simulate the 30-minute PV power forecast that would ordinarily come from an on-site cloud camera, three a very basic approaches are used. These are designed to represent a low and high benchmark, as well as a mid-range product.

Note that unlike a true forecast, these do not change over time.

The simulated forecasts created here are not in any way performing actual forecasting. Rather, they are simulating how closely to completely unconstrained generation a PV system could operate based on how good its forecasting technology is. As the forecast technology improves (from A to C), the PV output gets closer to what the PV output would be without constraints.

The three simulated forecasts are defined in the table below. Each forecast has two operating modes, based on whether the forecast window is classified as ‘clear’ or ‘not clear’. Specifically:

- A given 5-minute interval is classified as ‘clear’ if none of the 5-minute intervals in the forecast window into which the interval falls are cloudy, that is, the simulated PV output derived from the observed irradiance from the NTSR data is less than the simulated PV output derived from to the clearsky irradiance.
- A given 5-minute interval is classified as ‘not clear’ if any of the 5-minute intervals in the forecast window into which the interval falls are cloudy.

If the interval is ‘clear’ then the forecast will return the 100% of the clear sky PV output. If the interval is ‘not clear’, then the output depends on the type of forecast being simulated.

Table 3-1 Simulated Sky-Camera Forecasts

| | Conservative Forecast | Mid-Range Forecast | Precision Forecast |
|---|---|---|---|
| Description | A low benchmark, which is clearly within the capability of current technology | The most realistic of the three forecasts; closest to how a good, current technology forecast might work when constrained to the accuracy requirements of the Generator Performance Standards | A high-bar forecast; it represents a very good forecast, probably beyond the capability of the current technology |
| Forecast Window | 2 hours | 2 hours | 1 hour |
| Forecast Generation in ‘Not Clear’ Intervals | 15% of the clear sky PV Power | 50% of the 2-hour rolling minimum actual PV power | 90% of the 1-hour rolling minimum actual PV power |

The operation of these three different simulated forecasts on 3 pairs of days from the dataset is shown below.

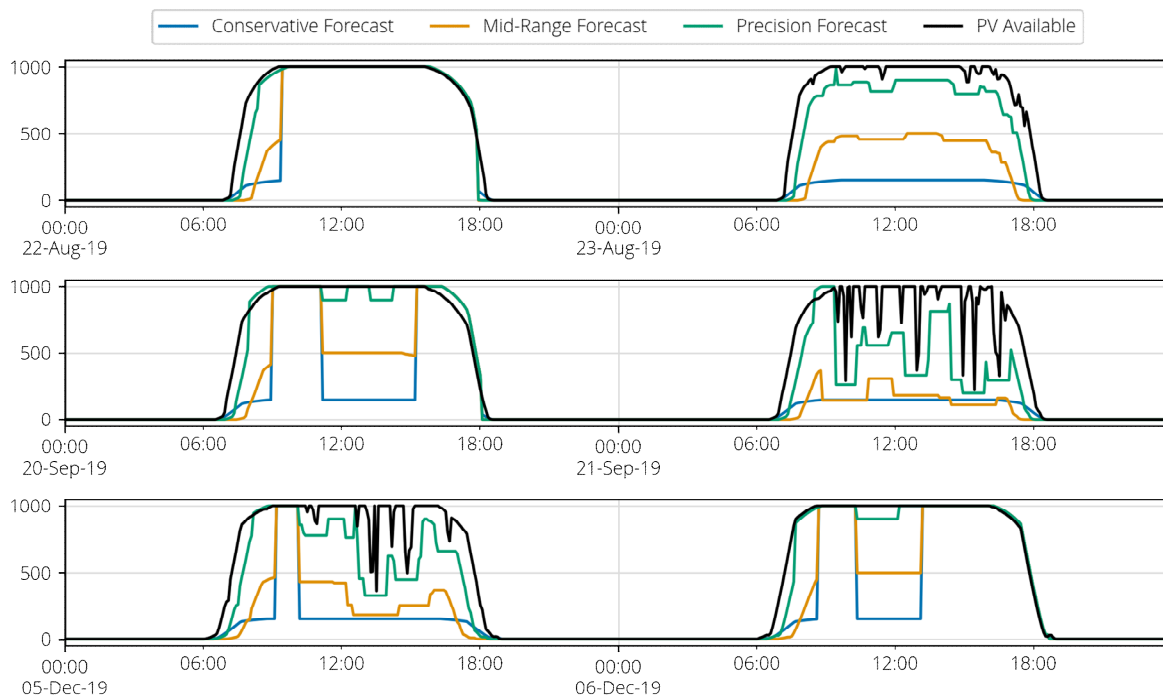


Figure 3-2 Simulated forecasts on selected days

3.2.4 Curtailment Calculation

Without storage, the calculation of curtailment is simple: power is dispatched up to the forecast, and no further. With storage, the system operates as per the figure below, which shows the battery charging at the beginning of the day, and discharging whenever the available PV falls below the sky camera forecast, and then emptying completely overnight. While the battery is charged, the PV is allowed to run above the sky camera forecast to the extent that the battery would be capable of compensating in the event of a sudden cloud. The output at which the PV is allowed to generate in this simulation is the amount that a generator would provide to PWC as a capacity forecast.

Batteries were assumed to have energy storage capacity equivalent to 30 minutes of generation at their maximum rated capacity and a round-trip efficiency of 95%.

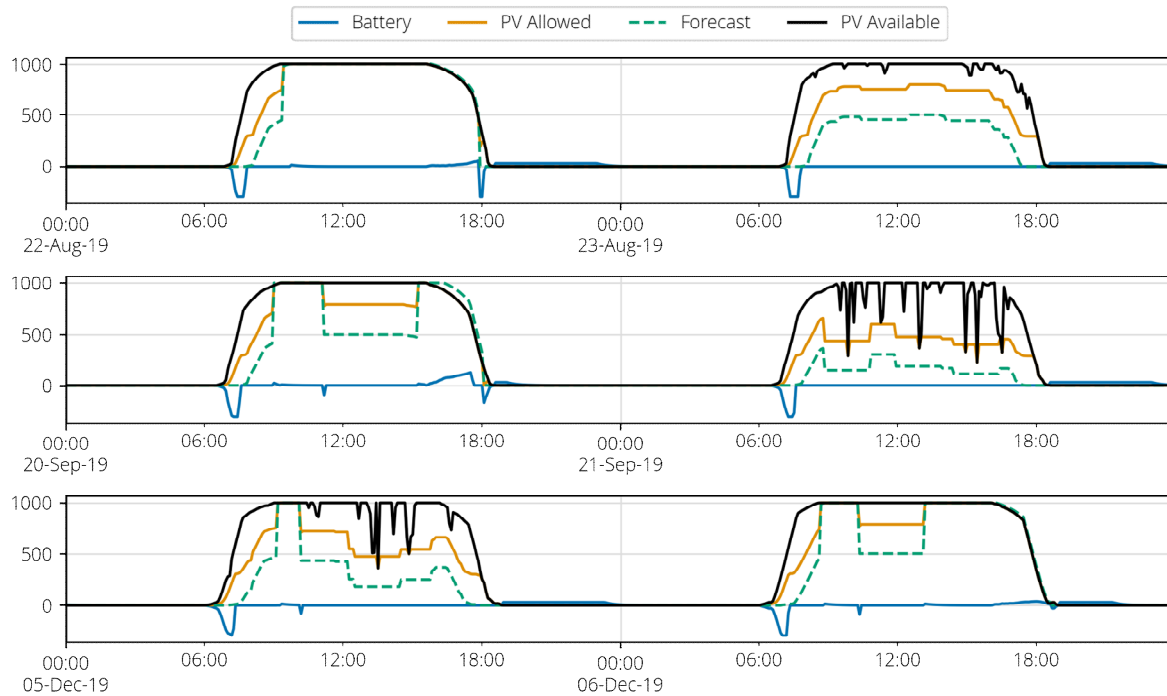


Figure 3-3 PV and battery operation illustration with the Mid-Range Forecast

The 'Forecast' line represents the simulated sky-camera forecast based on the Mid-Range Forecast simulation. The 'PV Allowed' line is the capacity forecast that the generator could confidently provide to PWC based on the sky-camera forecast and the available battery capacity at the given time.

3.2.5 NPV Calculation

The capital and operational expenditure of the PV and battery system is estimated using the following assumptions:

- PV system capital cost of \$1.39/W for PV [20].
- Battery capital cost of \$600/kWh, with one replacement required after 10 years [21].
- Battery annual operational cost of \$12/kWh [21].

Revenue from energy generation was calculated assuming an energy price of \$100/MWh, which is the approximate volume weighted price on the interim Northern Territory Energy Market (iNTEM) from 2016 to 2020. The annual system generation was calculated by summing and averaging PV and BESS output from the simulation described above carried out over all available data for each location. The revenue was calculated as the product of the total annual system generation and the energy price.

The system Net Present Value (NPV) was calculated for each battery size by summing the discounted expenditure and revenue over a project life of 20 years, using a real discount rate of 7%, a typical value for infrastructure projects [22].

3.3 RESULTS

The plot below shows the results of the analysis. As expected, smaller BESS sizes can be installed if higher accuracy forecasts are available, resulting in lower overall NPVs at each of

the four locations. However, the results clearly show that that the optimal BESS size reduces as the site moves further away from the tropical climate zone. This is consistent with the higher variability typically observed in these regions, as shown in Figure 2-1 and Figure 3-1. However, this effect is less pronounced for the more conservative forecasts.

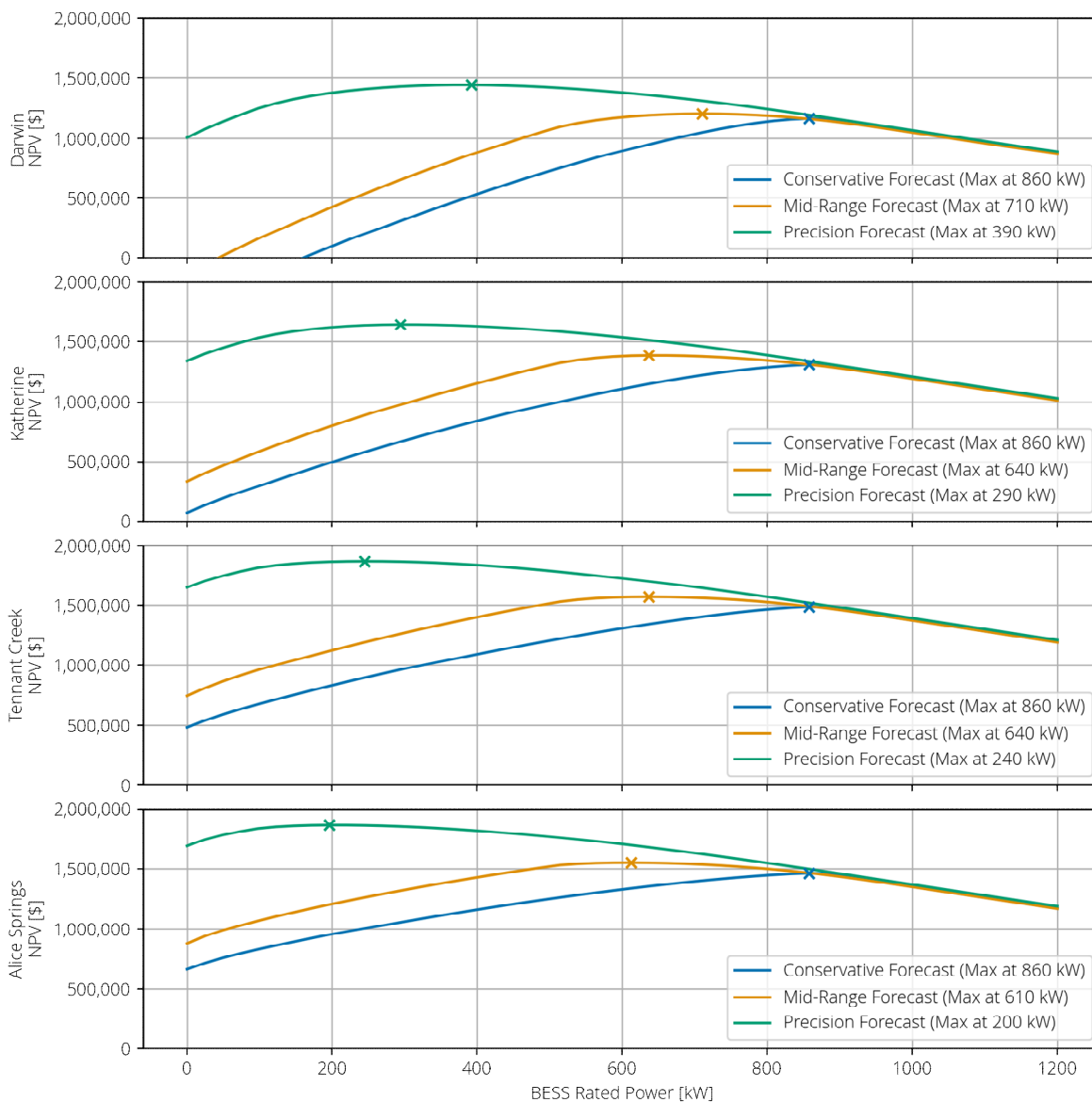


Figure 3-4 Optimal BESS sizing results

The results are summarised in the table below.

Table 3-2 Optimal BESS size for PV firming

| Location | Conservative Forecast | Mid-Range Forecast | Precision Forecast |
|----------------------|------------------------------|---------------------------|---------------------------|
| Darwin | 860 | 710 | 390 |
| Katherine | 860 | 640 | 290 |
| Tennant Creek | 860 | 640 | 240 |
| Alice Springs | 860 | 610 | 200 |

4 CONCLUSION

This analysis demonstrates the value of the high quality, high resolution data provided by the NTSR project.

The NTSR project data can improve forecasts of long-term solar resource variability by enabling site adaptation of satellite datasets and in doing so reduce the risk associated with potential PV installations. The application of this methodology increased the 1-year P90 annual GHI estimates at the different sites by approximately 14 to 28%. This illustrates the capacity of the ground station data to reduce the risk associated with long-term variability of solar resource for a given project.

The high resolution of the NTSR project data could assist developers in optimising BESS sizing to support forecasting at the level of accuracy required to meet current performance standards. An implementation of this methodology illustrated that the optimal BESS size increased with increasing the increasing short-term irradiance variability, as observed at the Top End stations. More conservative forecasts also resulted in larger BESS sizes required to maximise value. Assuming a 'mid-range' forecast accuracy representative of current cloud forecasting technology, the optimal BESS size ranges from 710 kW in Darwin to 610 kW in Alice Springs.

Further, the fact that these long-term and short-term variability analyses produced markedly different results for each of the four sites demonstrates the value of having consistent high quality ground stations distributed across the distinct climate zones across the NT.

It is intended that this study provide a template for future users of NTSR project data as the volume of available data increases. Future work could include: extending the long-term variability analysis to variables other than GHI; and applying the BESS optimisation methodology to a wider range of possible forecasts and/or stochastic models of forecast performance.

5 REFERENCES

- [1] A Langworthy, G Bourne, L Frearson, K Howard, A McKenzie & O Peake, "Northern Territory Roadmap to Renewables: Fifty per cent by 2030," 2017.
- [2] S Ong, A Atkins, B Herteleer, L McLeod, G Dickeson, H Norris & L Frearson, "Data of Value, Valuing Data: Open-Access Bankable Resource Data Project in Australia's Northern Territory," in *36th European Photovoltaic Solar Energy Conference and Exhibition*, 2019.
- [3] M Richter, C Tjengdrawira, J Vedde, M Green, L Frearson, B Herteleer, U Jahn & M Köntges, "Technical Assumptions used in PV Financial Models," International Energy Agency Photovoltaic Power Systems Programme, 2017.
- [4] J Polo, S Wilbert, JA Ruiz-Arias, R Meyer, C Gueymard, M Sári, L Martín, T Mieslinger, P Blanc, I Grant, J Boland, P Ineichen, J Remund, R Escobar, A Troccoli, M Sengupta, KP Nielsen, D Renne, N Geuder & T Cebecauer, "Preliminary survey on site-adaptation techniques for satellite-derived and reanalysis solar radiation datasets," *Solar Energy*, vol. 132, pp. 25-37, 2016.
- [5] M Sengupta, J Polo, C Gueymard & Y Xie, "Modelling Solar Radiation – Current Practices," in *Best Practices Handbook for the Collection and Use of Solar Resource Data for Solar Energy Applications: Second Edition*, NREL, 2017, p. ch. 4.
- [6] R Bouckaert, "Choosing between two learning algorithms based on calibrated tests," in *Proceedings of the Twentieth International Conference on Machine Learning (ICML-2003)*, Washington DC, 2003.
- [7] P Stackhouse, "NASA POWER | DocsNASA POWER | Docs | Methodology | Solar Insolation," NASA, 2020.

- [8] A Habte & M Sengupta, "Best Practices of Uncertainty Estimation for the National Solar Radiation Database (NSRDB 1998–2015)," NREL Conference Paper NREL/CP-5D00-70165, 2017.
- [9] M Suri & T Cebecauer, "Satellite-based Solar Resource Data: Model Validation Statistics Versus User's Uncertainty," in *ASES SOLAR 2014 Conference*, San Francisco, 2014.
- [10] Joint Committee for Guides in Metrology (JCGM), "Evaluation of measurement data — Guide to the expression of uncertainty in measurement," 2008.
- [11] T Cebecauer & M Suri, "Typical Meteorological Year data: SolarGIS Approach," *Energy Procedia*, vol. 69, p. 1958–1969, 2015.
- [12] L Ramírez, C Gueymard, D Renné, KP Nielsen, L Zarzalejo, S Wilbert & A Dobos, "Applying Solar Resource Data to Solar Energy Projects," in *Best Practices Handbook for the Collection and Use of Solar Resource Data for Solar Energy Applications: Second Edition*, NREL, 2017, p. ch. 8.
- [13] A Dobos, M Kasberg & P Gilman, "P50/P90 Analysis for Solar Energy Systems Using the System Advisor Model," in *NREL Conference Paper NREL/CP-6A20-54488*, 2012.
- [14] SY Kim, B Sapotta, G Jang, Y-H Kang & H-G Kim, "Prefeasibility Study of Photovoltaic Power Potential Based on a Skew-Normal Distribution," *Energies*, vol. 13, no. 3, p. 676, 2020.
- [15] CM Fernández Peruchena, L Ramírez, MA Silva-Pérez, V Lara, D Bermejo, M Gastón, S Moreno-Tejera, J Pulgar, J Liria, S Macías, R Gonzalez, A Bernardos, N Castillo, B Bolinaga, RX Valenzuela & LF Zarzalejo, "A statistical characterization of the long-term solar resource: Towards risk assessment for solar power projects," *Solar Energy*, vol. 123, pp. 29-39, 2016.
- [16] P Caballero, G Srinivasan & M Šúri, "How to calculate P90 (or other Pxx) PV energy yield estimates," SolarGIS, 2018.

- [17] G Dickeson, L McLeod, B Herteleer & L Frearson, "Constructing 1-Second Resolution Irradiance Datasets Using Clearness Index Samples," in *EU PVSEC 2019*, Marseille, 2019.
- [18] Power and Water Corporation, "Network Technical Code and Network Planning Criteria version 4," 2020.
- [19] W. F. Holmgren, C. W. Hansen and M. A. Mikofski, "pvlib python: a python package for modeling solar energy systems.," *Journal of Open Source Software*, vol. 3, no. 29, p. 884, 2018.
- [20] ARENA, "Large-scale solar," 2021.
- [21] K Mongird, V Viswanathan, P Balducci, J Alam, V Fotedar, V Koritarov & B Hadjerioua, "An Evaluation of Energy Storage Cost and Performance Characteristics," *Energies*, vol. 13, no. 13, p. 3307, 2020.
- [22] R Fernandez, "Review of discount rates used in economic evaluations," *Victoria's Economic Bulletin*, Vols. 3, April 2019, pp. 24-32, April 2019.